Available online at www.sciencedirect.com
SCIENCE DIRECT®
International Journal of Heat and Mass Transfer 47 (2004) 341–351
International Journal of HEAT and MASS TRANSFER
www.elsevier.com/locate/ijhmt

Numerical investigation of heat transfer characteristics of the heated blocks in the channel with a transversely oscillating cylinder

Wu-Shung Fu *, Bao-Hong Tong

Department of Mechanical Engineering, National Chiao Tung University, Hsinchu 30056, Taiwan, ROC

Received 24 January 2003; received in revised form 21 May 2003

Abstract

A numerical simulation is performed to study the influence of an oscillating cylinder on the heat transfer from heated blocks in a channel flow. An arbitrary Lagrangian–Eulerian kinematics description method is adopted to describe the flow and thermal fields. A penalty consistent finite element formulation is applied to solve the governing equations. The effects of Reynolds number, oscillating amplitude and oscillating frequency on the heat transfer characteristics of the heated wall are examined. The results show that the heat transfer from heated blocks is enhanced remarkably as the oscillating frequency of the cylinder is in lock-in region.

1. Introduction

A problem of forced convection in a channel flow with heated blocks is of practical importance and widely considered in the design of devices such as heat exchangers, and arrays of electronic components. Therefore, there is an urgent need for improving heat transfer performance of the heated blocks set in the channel.

Up to now, forced convection in a channel with heated blocks has been a subject of active research. Several studies [1–5] had investigated the heat transfer and flow characteristics in a channel with heated blocks. Furthermore, numerous methods including passive and active methods have been proposed to enhance the heat transfer from the heated blocks. One of these methods involves vortex generators or turbulence promoters installed in the channel and often used to enhance the heat transfer of the above subject. Liou et al. [6–8] curried out a series of numerical and experimental studies on the turbulent flows in a channel with turbulence promoters, and the results showed that the pitch ratio, Reynolds number and eccentric ratio affected the phenomena of separation, reattachment and heat transfer rate. Amon et al. [9,10] studied self-sustained oscillatory flows in communicating channels. The results indicated that self-sustained oscillations that resulted in very well mixed flows. On an equal pumping power basis, the heat transfer in communicating channels flows was higher than the one in a flat channel flow. Lin and Hung [11] studied transient forced convection heat transfer in a vertical rib-heated channel with a turbulence promoter, and found that the utilization of a turbulence promoter could effectively improve the heat transfer performance in the fully-developed region. Ghaddar et al. [12,13] investigate modulatory heat transfer enhancement in grooved channels by direct numerical simulation. The results show that resonant oscillatory forcing at modulatory amplitudes as small as 20% of the mean flow results in a doubling of transport as measured by a time, space-averaged Nusselt number. Myrum et al. [14,15] studied the effects of position of a vortex generator above or just downstream of a rib on the heat transfer in a heated duct. It was found that the maximum enhancement of heat transfer was about 30%. Garimella

* Corresponding author. Tel.: +886-3-572-7925; fax: +886-3-572-0634/572-7925.
E-mail address: wsfu@cc.nctu.edu.tw (W.-S. Fu).

0017-9310/$ - see front matter © 2003 Elsevier Ltd. All rights reserved.
doi:10.1016/S0017-9310(03)00303-X

Nomenclature

d	diameter of cylinder [m]
f_c	oscillating frequency of cylinder [s^{-1}]
F_c	dimensionless oscillating frequency of cylinder ($F_c = f_c d/u_c$)
h_c	distance from bottom side to center of cylinder [m]
h_e	height of the channel [m]
h_d	height of the block [m]
k	thermal conductivity
l_c	oscillating amplitude of cylinder [m]
L_c	dimensionless oscillating amplitude ($L_c = l_c/d$)
$\overline{Nu}$	periodic-averaged Nusselt number
$Nu_{overall}$	average Nusselt number of overall heated surface
$Nu_{surface}$	average Nusselt number of one surface of a block
Nu_X	local Nusselt number
p	dimensional pressure [$N\,m^{-2}$]
p_∞	reference pressure [$N\,m^{-2}$]
P	dimensionless pressure ($P = (p - p_\infty)/\rho u_0^2$)
Pr	Prandtl number ($Pr = \upsilon/\alpha$)
r	radius of cylinder [m]
R	dimensionless radial coordinate ($R = r/d$)
Re	Reynolds number ($Re = u_0 d/\upsilon$)
s	distance between two heated blocks [m]
t	time [s]
T	temperature [K]
T_H	temperature of high temperature region [K]
T_{mx}	local mean temperature [K]
T_0	temperature of inlet fluid [K]
u, v	velocities in x and y directions [$m\,s^{-1}$]
U, V	dimensionless velocities in X and Y directions ($U = u/u_0$, $V = v/u_0$)
u_0	velocities of inlet fluid [$m\,s^{-1}$]
v_c	oscillating velocity of cylinder [$m\,s^{-1}$]
V_c	dimensionless oscillating velocity of cylinder ($V_c = v_c/u_0$)
v_m	maximum oscillating velocity of cylinder [$m\,s^{-1}$]
V_m	dimensionless maximum oscillating velocity of cylinder ($V_m = v_m/u_0$)
$\hat{v}$	mesh velocity in y-direction [$m\,s^{-1}$]
$\hat{V}$	dimensionless mesh velocity in Y-direction ($\hat{V} = \hat{v}/u_0$)
w	length of channel [m]
w_1	length from inlet region to the center of the cylinder [m]
w_2	length from outlet region to the center of the cylinder [m]
w_3	length from the center of the cylinder to the first block [m]
w_b	dimensional length of the heated block [m]
x, y	dimensional Cartesian coordinates [m]
X, Y	dimensionless Cartesian coordinates ($X = x/h_e$, $Y = y/h_e$)

Greek symbols

α	thermal diffusivity [$m^2\,s^{-1}$]
Φ	computational variables
λ	penalty parameter
υ	kinematics viscosity [$m^2\,s^{-1}$]
θ	dimensionless temperature ($\theta = (T - T_0)/(T_H - T_0)$)
θ_{mX}	dimensionless local mean temperature
ρ	density [$kg\,m^{-3}$]
τ	dimensionless time ($\tau = tu_0/h_e$)
τ_p	dimensionless time of one oscillating cycle
Ψ	dimensionless stream function

Others

$\|\,\|$	absolute value
$\bar{}$	time average per periodic cycle

and Eibeck [16] examined the effect of protrusion of a vortex generator on heat transfer from an array of discrete heated elements. The maximum heat transfer enhancement was about 40%. Iyer and Kakac [17] investigated the instability and heat transfer in grooved channel flow. The results showed that beyond a critical Reynolds number, the heat transfer rate could be enhanced. Ortega [18] studied asymmetric oscillator by numerical method, and try to understand the resonance phenomenon for the asymmetric oscillator. Chen and Wang [19] adopted experimental and numerical methods to study the forced convective flow in a channel with heated blocks in tandem. The results compared the variations of the Sherwood number along the heated surfaces between the laminar and turbulent convection cases and discussed the effect of the block spacing on heat transfer. Wu and Perng [20] studied a numerically investigated heat transfer enhancement in a horizontal block-heated channel an oblique plate installed. The maximum increase of average Nusselt number was 39.5% when the oblique angle was $\pi/3$. Herman and Kang [21] investigated the heat transfer enhancement in a grooved channel with curved vanes. The results showed that flow oscillations contributed to heat transfer enhancement.

Most methods mentioned above are passive, and the improvement of heat transfer rate and the effective range are limited. Therefore, an effective method proposed in

this study is to utilize an oscillating cylinder suspended in the channel and in crossflow to cause the occurrence of flow vibration and vortex shedding, which could enhance the heat transfer rate of the heated blocks set in the channel walls.

The subject of the present work is therefore to investigate the influence of the flow passing over the oscillating cylinder on the heated blocks in the channel. The subject mentioned above belongs to the class of moving boundary problems, and the arbitrary Lagrangian–Eulerian (ALE) method modified by Fu and Yang [22] is suitably adopted to solve this problem. The heat transfer characteristics along the heated blocks are presented in detail. The mainly effects of Reynolds number, oscillating amplitude and oscillating frequency on the flow structures and heat transfer characteristics are investigated.

2. Physical model

The physical model used in this study is shown in Fig. 1. A two-dimensional channel with height h_e and length w is used to simulate this problem. An insulated cylinder of diameter d is set centrally within the channel. The distances from the inlet and outlet of the channel to the center of cylinder are w_1 and w_2, respectively. The distance from the center of the cylinder to the front surface of the first block is w_3. The height and length of the heated blocks are h_b and w_b, respectively. The distance between the blocks is s. The numbers of I, II, III and IV of the blocks are arranged from front to rear position. In this study h_e/d is 4, h_b/d is 0.8, w_b/d is 2, s/d is 1. The inlet velocity u_0 and temperature T_0 of the fluid are uniform. The temperature of the heated blocks is T_H which is higher than T_0. The wall of the channel is insulated. Initially, the cylinder is stationary at the position of the center of the channel and the fluid flows steadily. The distance from the wall of the channel to the center of the cylinder is h_c. As the time $t > 0$, the cylinder is in oscillating motion normal to the inlet flow with amplitude l_c. The oscillating velocity of the cylinder is $v_c = 2\pi l_c \cos(2\pi f_c t)$. The oscillating cylinder and the flow then affects each other, and the variations of the flow field become time-dependent and are classified into a class of moving boundary problems. As a result, the ALE method is properly utilized to analyze this problem.

For facilitating the analysis, the following assumptions are made.

(1) The fluid is air and the flow field is two-dimensional, incompressible and laminar.
(2) The fluid properties are constant and the effect of the gravity is neglected.
(3) The no-slip condition is held on the interfaces between the fluid and cylinder.

Based upon the characteristics scales of d, u_0, ρu_0^2 and T_0, the dimensionless variables are defined as follows:

$$X = \frac{x}{d}, \quad Y = \frac{y}{d}, \quad U = \frac{u}{u_0}, \quad V = \frac{v}{u_0}, \quad \hat{V} = \frac{\hat{v}}{u_0},$$
$$V_c = \frac{v_c}{u_0}, \quad L_c = \frac{l_c}{d}, \quad H_c = \frac{h_c}{d}, \quad F_c = \frac{f_c d}{u_0}, \quad P = \frac{p - p_\infty}{\rho u_0^2},$$
$$\tau = \frac{t u_0}{d}, \quad \theta = \frac{T - T_0}{T_H - T_0}, \quad Re = \frac{u_0 d}{\upsilon}, \quad Pr = \frac{\upsilon}{\alpha}, \tag{1}$$

where $\hat{v}$ is the mesh velocity, v_c, f_c, h_c and l_c are the oscillating velocity, the oscillating frequency, the position and the oscillating amplitude of the cylinder, respectively.

According to the above assumptions and dimensionless variables, the dimensionless ALE governing equations are expressed as:

Continuity equation

$$\frac{\partial U}{\partial X} + \frac{\partial V}{\partial Y} = 0, \tag{2}$$

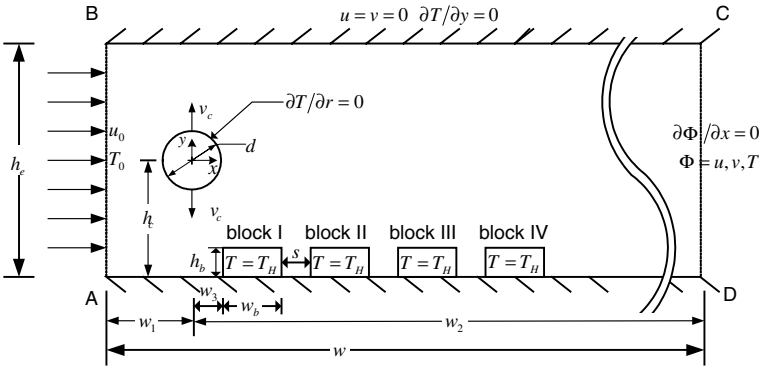

Fig. 1. Physical model.

Momentum equation

$$\frac{\partial U}{\partial \tau}+U\frac{\partial U}{\partial X}+(V-\hat{V})\frac{\partial U}{\partial Y} =-\frac{\partial P}{\partial X}+\frac{1}{Re}\left(\frac{\partial^2 U}{\partial X^2}+\frac{\partial^2 U}{\partial Y^2}\right), \tag{3}$$

$$\frac{\partial V}{\partial \tau}+U\frac{\partial V}{\partial X}+(V-\hat{V})\frac{\partial V}{\partial Y}=-\frac{\partial P}{\partial Y}+\frac{1}{Re}\left(\frac{\partial^2 V}{\partial X^2}+\frac{\partial^2 V}{\partial Y^2}\right), \tag{4}$$

Energy equation

$$\frac{\partial \theta}{\partial \tau}+U\frac{\partial \theta}{\partial X}+(V-\hat{V})\frac{\partial \theta}{\partial Y}=\frac{1}{Re\ Pr}\left(\frac{\partial^2 \theta}{\partial X^2}+\frac{\partial^2 \theta}{\partial Y^2}\right), \tag{5}$$

As the time $\tau > 0$, the boundary conditions are as follows:

On the inlet surface AB

$$U=1,\quad V=0,\quad \theta=0, \tag{6}$$

On the wall of channel

$$U=0,\quad V=0,\quad \frac{\partial \theta}{\partial Y}=0, \tag{7}$$

On the surfaces of the block I, II, III, IV

$$U=0,\quad V=0,\quad \theta=1, \tag{8}$$

On the outlet surface CD

$$\frac{\partial U}{\partial X}=0,\quad \frac{\partial V}{\partial X}=0,\quad \frac{\partial \theta}{\partial X}=0, \tag{9}$$

On the interfaces between the fluid and cylinder

$$U=0,\quad V=V_c,\quad \frac{\partial \theta}{\partial R}=0. \tag{10}$$

3. Numerical method

The governing equations and boundary conditions are solved through the Galerkin finite element formulation and a backward scheme is adopted to deal with the time terms of the governing equations. The pressure is eliminated from the governing equations using the consistent penalty method. The velocity and temperature terms are expressed as quadrilateral element and eight-node quadratic Lagrangian interpolation function. The Newton–Raphson iteration algorithm is utilized to simplify the nonlinear terms in the momentum equations. The discretion processes of the governing equations are similar to the one used in Fu and Yang [22].

A brief outline of the solution procedures are described as follows:

(1) Determine the optimal mesh distribution and number of the elements and nodes.
(2) Solve the values of the U, V and θ at the steady state and regard them as the initial values.
(3) Determine the time step $\Delta\tau$ and the mesh velocity $\hat{V}$ of the computational meshes.
(4) Update the coordinates of the nodes and examine the determinant of the Jacobian transformation matrix to ensure the one to one mapping to be satisfied during the Gaussian quadrature numerical integration.
(5) Solve Eq. (11), until the following criteria for convergence are satisfied:

$$\left|\frac{\Phi^{m+1}-\Phi^{m}}{\Phi^{m+1}}\right|_{\tau+\Delta\tau}<10^{-3},\quad \text{where } \Phi=U,V,\ \text{and } \theta. \tag{11}$$

(6) Continue the next time step calculation until periodic solutions are attained.

4. Results and discussion

The working fluid is air with $Pr=0.71$. The main parameters of Reynolds number Re, oscillating amplitude L_c and oscillating frequency F_c are examined and the combinations of these parameters are tabulated in Table 1.

In the channel, the thermal boundary layer grows in the downstream direction gradually. In order to describe the wall heat transfer in the channel region realistically, it is necessary to define the local mean temperature T_{mx} of the stream as:

$$T_{mx}=\frac{1}{\bar{u}\cdot h_e}\int_0^h uT\,dy,\quad \text{where } \bar{u}=\int_0^h u\,dy. \tag{12}$$

The dimensionless variable θ_{mX} is defined as

$$\theta_{mX}=\frac{T_{mx}-T_0}{T_H-T_0}. \tag{13}$$

The local Nusselt number is calculated by the following equation:

Table 1
Parameter combinations

Case	F_c	L_c	Re
1	0.1	0.1	250
2	0.2	0.1	250
3	0.4	0.1	250
4	0.2	0.05	250
5	0.2	0.2	250
6	0.2	0.4	250
7	0.2	0.1	100
8	0.2	0.1	500

$$Nu_X = \left(-\frac{\partial\theta}{\partial n}\bigg|_{\text{block surface}} \right) \frac{1}{1-\theta_{mX}}. \quad (14)$$

The time-averaged local Nusselt number per oscillatory cycle is defined by

$$\overline{Nu} = \frac{1}{\tau_p}\int_0^{\tau_p} Nu_X \, d\tau \quad \text{where } \tau_p \text{ is a period of the cycle.} \quad (15)$$

The average Nusselt number along one surface of a heated block is found as follows:

$$Nu_{\text{surface}} = \frac{1}{X_s}\int_{\text{surface}} Nu_X \, dX,$$

where X_s is length of heated surface. (16)

The time-average Nusselt number along one surface of a heated block per cycle period is expressed as follows:

$$\overline{Nu_{\text{surface}}} = \frac{1}{\tau_p}\int_0^{\tau_p} Nu_{\text{surface}} \, d\tau. \quad (17)$$

The overall Nusselt number of the four heated blocks is defined by

$$Nu_{\text{overall}} = \frac{1}{4(w_b + 2h_b)} \sum_{\text{block1}}^{\text{block4}} Nu_{\text{surface}}. \quad (18)$$

The time-average overall Nusselt number of the four heated blocks per cycle period is defined by

$$\overline{Nu_{\text{overall}}} = \frac{1}{\tau_p}\int_0^{\tau_p} Nu_{\text{overall}} \, d\tau. \quad (19)$$

For matching the boundary conditions at the inlet and outlet of the channel mentioned above, the dimensionless lengths from the inlet and outlet to the cylinder are determined by numerical tests and equal to 15.0 and 120.0, respectively. To obtain an optimal computational mesh, three different nonuniform distributed elements, which provide a finer element resolution near the cylinder and walls, are used for the mesh tests. Fig. 2(a) and (b), show the velocity profiles along the line through the center of the cylinder and parallel to the Y-axis at the steady state for $Re = 500$, respectively. Based upon the results, the computational mesh with 6700 elements, which is corresponding to 20216 nodes, is used for all cases in this study. In addition, an implicit scheme is employed to deal with the time differential terms of the governing equations. After the time step test, the time step $\Delta\tau = 0.01$ is chosen for all cases in this study.

The dimensionless stream function Ψ is defined as

$$U = \frac{\partial\Psi}{\partial Y}, \quad V = -\frac{\partial\Psi}{\partial X}. \quad (20)$$

Fig. 3 shows a comparison of the present results with those of Kim [22] under the same situation, both the results show good agreement.

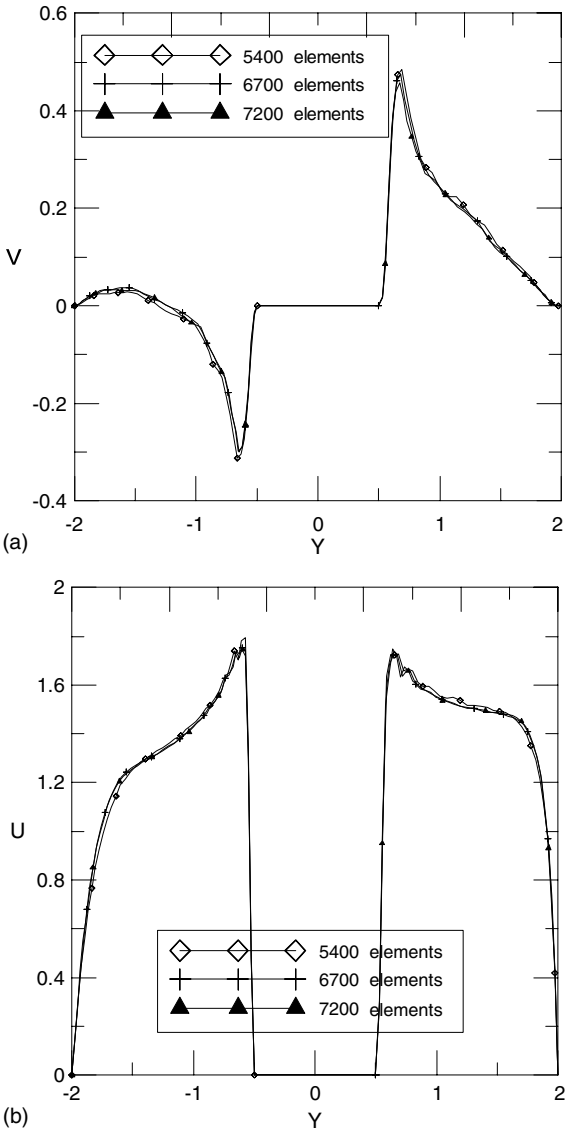

Fig. 2. Comparison of the velocity profiles along the line through the center of the cylinder and parallel the Y-axis for different mesh.

For a better understanding of the phenomena around the oscillating cylinder and heated blocks, the flow and thermal fields close to the oscillating cylinder and heated blocks are illustrated in the following figures. The variations of the streamlines under $Re = 250$, $L_c = 0.2$ and $F_c = 0.2$ are indicated in Fig. 4. Fig. 4(a) shows the streamlines in the empty channel with heated blocks at steady state. Due to the obstruction of the first block, the streamlines begin to deflect at upstream of the first block and the fluid is accelerated upward. Therefore, a small vortex is formed on the top surface of the first

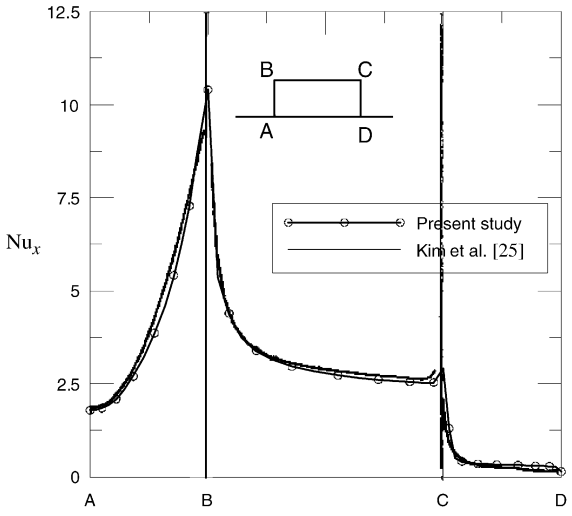

Fig. 3. Comparison of the present study with the existing study.

block. At the same time, other larger vortex downstream of the last heated block is observed. Weak clockwise vortices are formed within the grooves, which are similar to the cavity flow. These vortices are the main impediment for the heat transfer from the heated blocks.

At the time $\tau = 0$, shown in Fig. 4(b), the cylinder is stationary and the flow is steady. The fluid flows upward into the narrow space between the first block and cylinder, the fluid is accelerated more drastically due to the contraction effect. Besides, due to the effect of the cylinder, a vortex forming on the top surfaces of the blocks is larger than that of the channel without the cylinder installed shown above and reaches the fourth block. As a result, the heat transfer from the top surface of the heated blocks of Fig. 4(b) situation is worse than that of Fig. 4(a) situation.

As the time $\tau > 0$, the cylinder starts to oscillate with the oscillating velocity $V_c = 2\pi F_c L_c \cos(2\pi F_c \tau)$, where the oscillating frequency F_c is 0.2 and the oscillating amplitude L_c is 0.2. Fig. 4(c) shows the cylinder that has moved upward to the maximum amplitude. The cylinder squeezes the fluid near the upper region of the channel and the fluid near the bottom surface of the cylinder replenishes the vacant space induced by the oscillating cylinder. As a result, the original vortex behind the cylinder is shed from the cylinder and moves downstream. Afterward, the cylinder moves downward direction immediately and the Fig. 4(d) shows the cylinder on the way to move downward. The fluid near the top surface of the cylinder simultaneously replenishes the vacant space created by the movement of the cylinder, and the cylinder presses the fluid near the bottom surface of the cylinder. Then a new vortex is formed gradually behind the cylinder. The oscillating cylinder influences the formation of large vortex on the top surfaces of the blocks. As shown in the Fig. 4(e), because of the vortex shedding and the oscillating motion of the cylinder, the large vortex on the top surfaces of heated blocks is difficult to maintain its original state, which causes the large vortex to be split into small vortices and move downstream with the flow. The cylinder reaches the lowest amplitude. A new vortex forms on the top surface of the first block and pushes the existing vortices to the downstream as the cylinder is on the way to move upward shown in Fig. 4(f). When the cylinder returns to the center of the channel with the maximum upper velocity, the cylinder completes the first oscillation cycle, and the cycle time τ is 5.

As the time increases, shown in Fig. 4(g), during the second oscillation cycle and the same situation as the Fig. 4(f), the vibrational flow not only pushes the vortices generated on the top surfaces of the blocks to the downstream continually but also starts to affect the

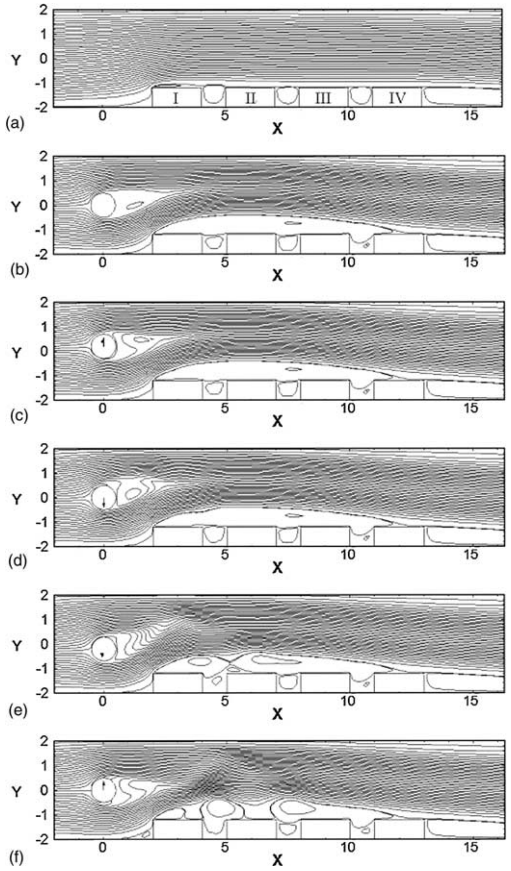

Fig. 4. The transient developments of streamlines for case 2. (a) Empty channel, (b) $\tau = 0$, (c) $\tau = 1.25$, (d) $\tau = 2.5$, (e) $\tau = 3.75$, (f) $\tau = 5$, (g) $\tau = 10$, (h) $\tau = 115$, (i) $\tau = 116.25$, (j) $\tau = 117.5$, (k) $\tau = 118.75$, (l) $\tau = 120$.

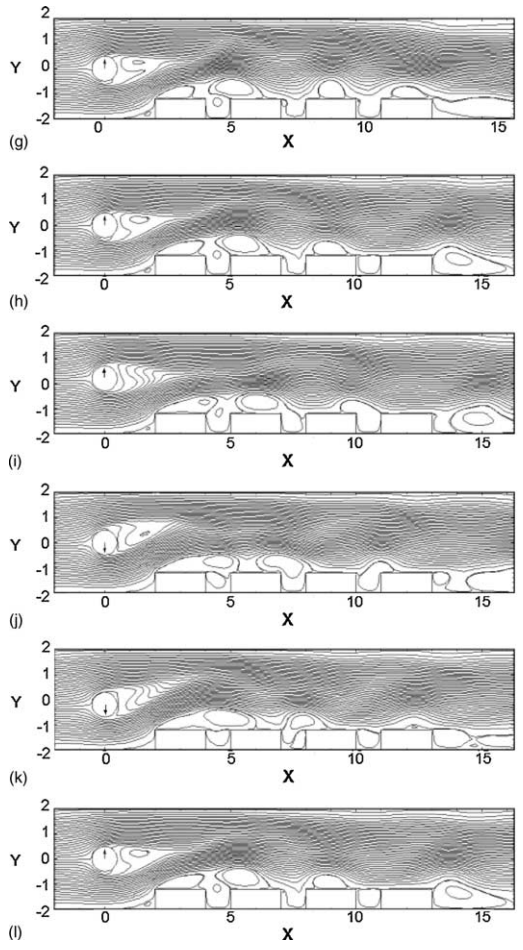

Fig. 4 (*continued*)

vortices between the blocks and behind the last block gradually.

Fig. 4(h)–(l) show the variations of the streamlines during one steadily periodic cycle. As shown in these figures, the new vortices on the heated blocks are generated periodically by the oscillating cylinder and push other vortices to the downstream continually. The vortices between the blocks form and are ejected alternately. Comparing Fig. 4(h) and (l), the streamlines are identical which means that the variations of the flow become a steadily periodic motion with time.

The distributions of local Nusselt number Nu_X on the different surfaces of the blocks in a channel with a stationary cylinder and with an oscillating cylinder during one period are shown in Fig. 5. The situations of the different times in Fig. 5 correspond to those shown in the Fig. 4(h)–(l). The shedding vortices affect the local heat transfer from blocks remarkably due to the movement of vortices. However, the influence of vortex shedding is not obvious on the first block.

The variations of the overall average Nusselt number Nu_{overall} with time of all blocks for the situation of $Re = 250$, $F_c = 0.2$ and $L_c = 0.2$ (case A) are shown in Fig. 6 and compare the Nusselt number with the same situations of an empty channel (case B) and a channel with a stationary cylinder as the flow in steady state (case C). In the beginning, the difference between the cases of A and C is small. As the time increases, the effect of the oscillating cylinder on the heat transfer of case A is apparent gradually. Finally, the variation of the heat transfer approaches a periodic state with time ($\tau \geqslant 80$). The increase of the heat transfer of case A compared with those of cases B and C is more than 60% and 120%, respectively.

When the oscillating frequency approaches the natural shedding frequency, it would cause the lock-in phenomenon to happen [23]. For a flow passing through a stationary cylinder, the natural frequency of vortex shedding F_c is about 0.2 over a range of Reynolds number from 2×10^2 to 10^4 [24]. The effects of the oscillating frequency on the heat transfer of each surface of the blocks are shown in Fig. 7 for the $L_c = 0.1$ and $Re = 250$ situation. Comparing with the stationary cylinder, the average Nusselt numbers $\overline{Nu}_{\text{surface}}$ along each surface of the heated blocks are enhanced substantially. It can be observed that as the oscillating frequency is in the lock-in regime ($F_c = 0.2$), the heat transfer of each surface, except for the front surface of the first block, is greater than those of other frequencies situations obviously. Conversely, when the values of F_c are equal to 0.1 and 0.4, because of the flow in the unlock-in flow, the enhancement for the heat transfer rate of these flows are not as significant as that in the lock-in regime.

Fig. 8 shows the effects of the oscillating amplitude on the heat transfer of each surface of the blocks for the $F_c = 0.2$ and $Re = 250$ situation. Comparing with the stationary cylinder, the increase of the surface average Nusselt numbers $\overline{Nu}_{\text{surface}}$ along each surface of the heated blocks is significant. Therefore, the effect of the oscillating amplitude on the heat transfer from the heated block is remarkable as the oscillating amplitude is larger than 0.1.

The effects of the Reynolds number on the heat transfer from each surface of the blocks for the $L_c = 0.1$ and $F_c = 0.2$ situation are shown in Fig. 9. The higher the Reynolds number is, the velocity and disturbance of fluid are quicker and more drastic, respectively. Thus the heat transfer rate is enhanced remarkably with the increment of the Reynolds number.

Table 2 shows the comparison of the time average overall Nusselt number $\overline{Nu}_{\text{overall}}$ of the heated blocks in the channel installed with the oscillating cylinder with those of having no installation of the oscillating cylinder. The results show the heat transfer could be improved by the oscillating cylinder just only as the oscillating frequency is in the lock-in region.

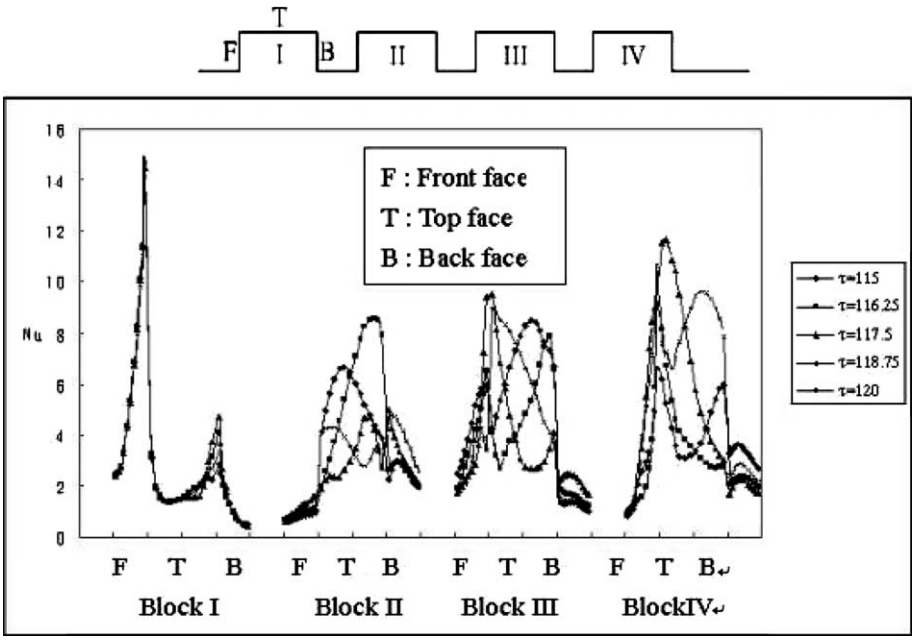

Fig. 5. The distributions of the local Nusselt number on the different surfaces of the blocks for case 2.

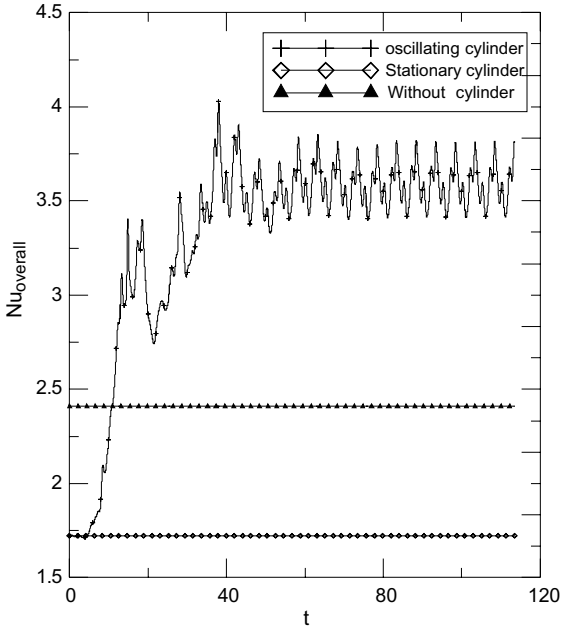

Fig. 6. Vibration of the overall-average Nusselt number with time.

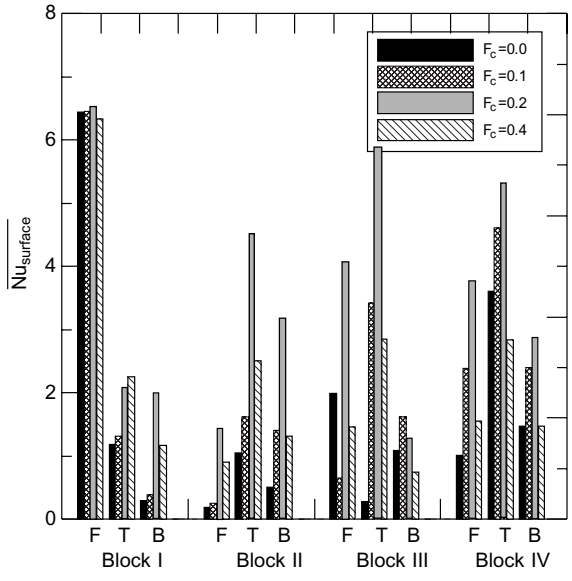

Fig. 7. The variations of average Nusselt number of each block for various frequencies under $L_c = 0.1$, $Re = 250$ situation.

Fig. 10 shows the pictures of flow visualization for the $Re = 267$ situation. The Ni–Cr wire on which paraffin was applied and evaporated paraffin instantaneously by resistive heating to generate white smoke is installed at the distance of 0.8D downstream from the center of the cylinder, and the oscillating cylinder is controlled by a stepper motor. The experimental study is intended to simulate as closely as possible to the above

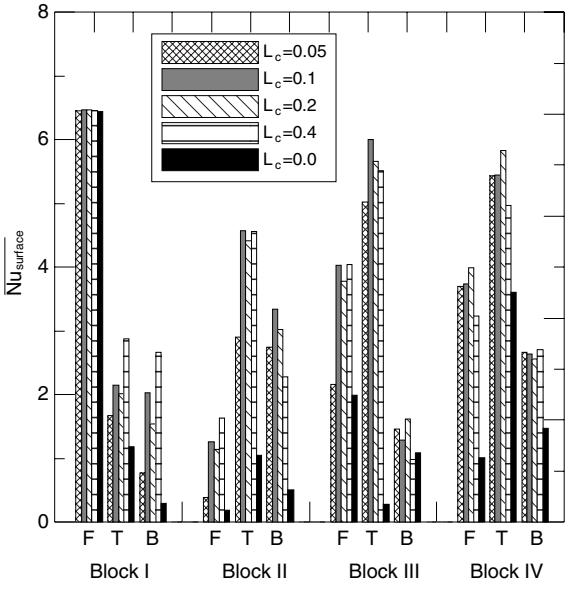

Fig. 8. The variations of overall Nusselt number average Nusselt number of each blocks for various oscillating amplitudes under $F_c = 0.2$, $Re = 250$ situation.

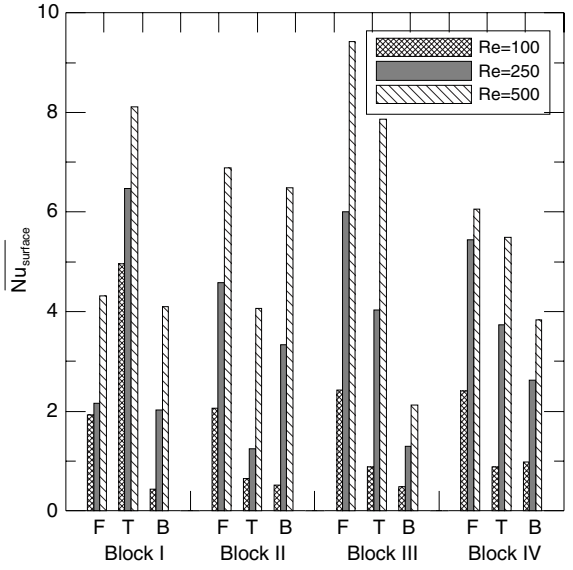

Fig. 9. The variations of overall Nusselt number average Nusselt number of each blocks for various Reynolds number under $F_c = 0.2$, $L_c = 0.1$ situation.

numerical simulation model, however, the blocks are not equipped with the heat sources. Fig. 10(a) shows the streaklines in the channel under without cylinder situation. As the streaklines develop over the blocks, they are close to the top surfaces of the blocks. These phenomena are similar to the numerical results shown in Fig. 4(a). Fig. 10(b) shows the phenomena of the streaklines developing over the blocks under the stationary cylinder installed in the channel situation. Since the space between the cylinder and the first block in contracted, the streaklines passing this space is like to pass expansion region. The streaklines are no longer close to the top surfaces of the blocks as shown in Fig. 10(a), which indicates a circulation forming on the top surface of the blocks and is similar to the numerical results shown in Fig. 4(b). Fig. 10(c)–(f) indicate the periodical phenomena of the cylinder oscillating under $Re = 267$ and $F_c = 0.2$ situation. A small vortex observed on the top surface of second block (Fig. (c)) moves downstream continuously ((c) → (d) → (e) → (f)) which are similar to these results of Figs. 4(g)–(k) quantitatively.

Table 2
Compare the $\overline{Nu_{overall}}$ in the channel with the oscillating cylinder with those without oscillating cylinder

Case	$\frac{(\overline{Nu_{overall}})_{oscillating\ cylinder} - (\overline{Nu_{overall}})_{empty\ channel}}{(\overline{Nu_{overall}})_{empty\ channel}}(\%)$
1	−0.9
2	62
3	−5
4	33
5	59
6	60
7	−7
8	116.5

5. Conclusions

The heat transfer characteristics of the heated blocks in the channel with a transversely oscillating cylinder in a cross flow are investigated numerically. Some conclusions are summarized as follows:

1. The heat transfer rate could be improved substantially as the cylinder oscillating in the lock-in region.
2. The influence of oscillating amplitude on the heat transfer rate is not obvious under the lock-in region.
3. The heat transfer rate is increased when the Reynolds number increases.

Acknowledgements

The support of this work by the National Science Council of Taiwan, ROC, under contract NSC89-2212-E009-019 is gratefully acknowledged.

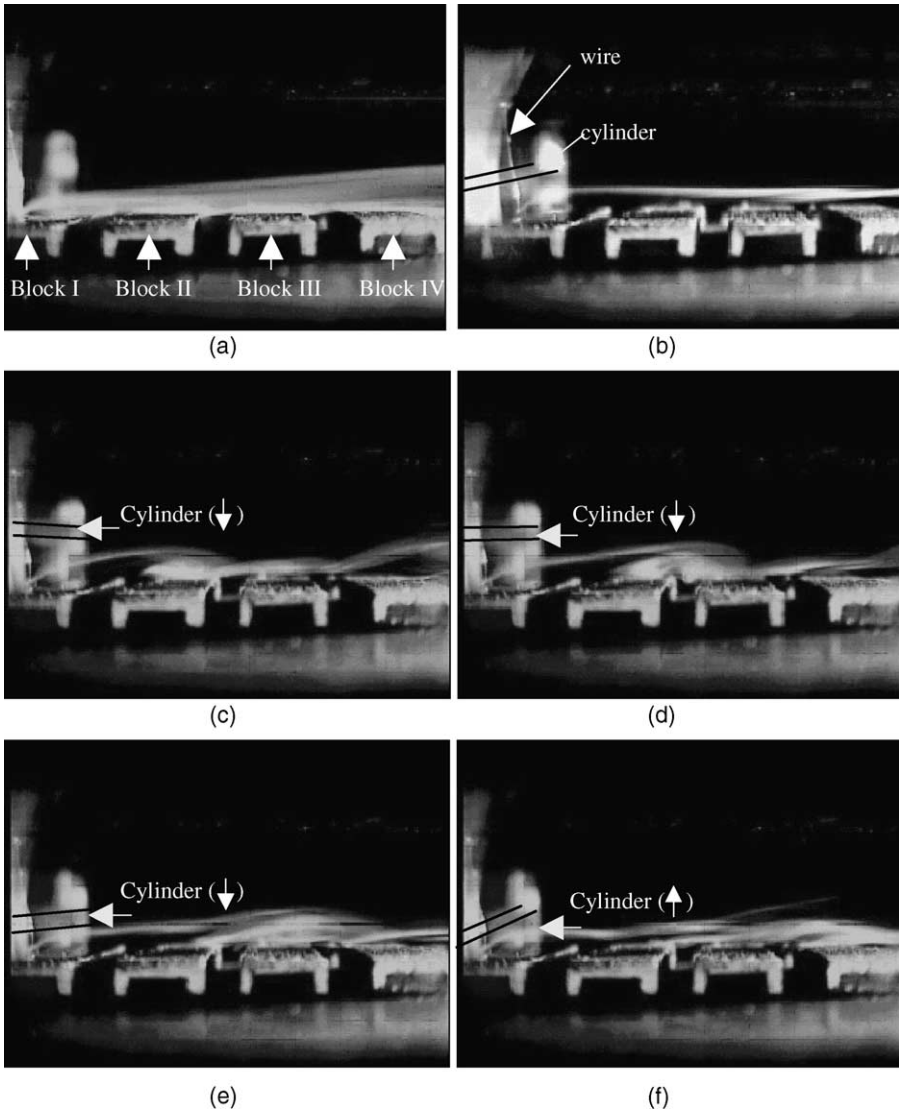

Fig. 10. The flow visualization.

References

[1] E.M. Sparrow, S.B. Vemuri, D.S. Kadle, Enhanced and local heat transfer, pressure drop, and flow visualization, Int. J. Heat Mass Transfer 26 (1983) 689–699.

[2] Y. Wang, A.J. Ghajar, Effect of component geometry and layout on flow distribution for surface mounted electronic components: a smoke flow visualization study, ASME HTD-Vol. 183, Heat Transfer Enhancement in Electronics Cooling, 1991, pp. 25–31.

[3] B.A. Jubran, S.A. Swiety, M.A. Hamdan, Convective heat transfer and pressure drop characteristics of various array configurations to simulate the cooling of electronic modules, Int. J. Heat Mass Transfer 39 (1996) 3519–3529.

[4] T.J. Young, K. Vafai, Convective flow and heat transfer in a channel containing multiple heated obstacles, Int. J. Heat Mass Transfer 41 (1998) 3279–3298.

[5] T.-C. Hung, C.-S. Fu, Conjugate heat transfer analysis for the passive enhancement of electronic cooling through geometric modification in a mixed convection domain, Num. Heat Transfer A 35 (1999) 519–535.

[6] T.M. Liou, Y. Chang, D.W. Hwang, Experimental and computational study of turbulent flows in a channel with two pairs of turbulence promoters in tandem, J. Fluids Eng. Trans. ASME 112 (1990) 302–310.

[7] T.M. Liou, W.B. Wang, Y.J. Chang, Holographic interferometry study of spatially periodic heat transfer in a channel with ribs detached from one wall, Trans. ASME 117 (1995) 199.

[8] J.J. Hwang, T.M. Liou, heat transfer in a rectangular channel with perforated turbulence promoters using holographic interferometry measurement, Int. J. Heat Mass Transfer 38 (17) (1995) 3197–3207.
[9] C.H. Amon, B.B. Mikic, Numerical prediction of convective heat transfer in self-sustained oscillatory flows, J. Thermophys. Heat Transfer 4 (2) (1990) 239–246.
[10] D. Majumdar, C.H. Amon, Heat and momentum transport in self-sustained oscillatory viscous flows, J. Heat Transfer-Trans. ASME 114 (4) (1992) 866–873.
[11] H.H. Lin, Y.H. Hung, Transient forced convection heat transfer in a vertical rib-heated channel using a turbulence promoter, Int. J. Heat Mass Transfer 36 (6) (1993) 1553–1571.
[12] N.K. Ghaddar, M. Magen, B.B. Kikic, A.T. Patera, Numerical investigation of incompressible flow in grooved channels. I. Stability and self-sustained oscillations, J. Fluid Mech. 163 (1986) 99–127.
[13] N.K. Ghaddar, M. Magen, B.B. Kikic, A.T. Patera, Numerical investigation of incompressible flow in grooved channels. II. Resonance and oscillatory heat transfer enhancement, J. Fluid Mech. 168 (1986) 541–567.
[14] T.A. Myrum, S. Acharya, S. Inamdar, A. Mehrotra, Vortex generator induced heat transfer augmentation past a rib in a heated duct air flow, J. Heat Transfer 114 (1992) 280–284.
[15] T.A. Myrum, X. Qiu, S. Acharya, Heat transfer enhancement in ribbed duct using vortex generators, Int. J. Heat Mass Transfer 36 (1993) 3497–3508.
[16] S.V. Garimella, P.A. Eibeck, Enhancement of single phase convective heat transfer from protruding elements using vortex generators, Int. J. Heat Mass Transfer 34 (1991) 2431–2433.
[17] R.S. Iyer, S. Kakac, Instability and heat transfer in grooved channel flow, J. Thermophys. Heat Transfer 11 (3) (1997) 437–445.
[18] R. Ortega, Asymmetric oscillators and twist mappings, J. London Math. Soc. 53 (1996) 325–342.
[19] Y.M. Chen, K.C. Wang, Experimental study on the forced convective flow in a channel with heated blocks on tandem, Exp. Thermal Fluid Sci. 16 (1997) 286–298.
[20] H.W. Wu, S.W. Perng, Effect of an oblique plate on the heat transfer enhancement of mixed convection over heated blocks in a horizontal channel, Int. J. Heat Mass Transfer 42 (1999) 1217–1235.
[21] C. Herman, E. Kang, Heat transfer enhancement in a grooved channel with curved vanes, Int. J. Heat Mass Transfer 45 (2002) 3741–3757.
[22] S.Y. Kim, B.H. Kang, Y. Jaluria, Thermal interaction between isolated heated electronic components in pulsating channel flow, Num. Heat transfer 34 (1998) 1–21.
[23] R.K. Shah, A.L. London, Laminar flow forced convection in ducts, Academic Press, 1978.
[24] C.-H. Cheng, H.-N. Chen, W. Aung, Experimental study of the effect of transverse oscillation on convection heat transfer from a circular cylinder, J. Heat Transfer 119 (1997) 474–482.